Spatial Computational Hepatic Molecular Biomarker Reveals LSECs Role in Mid Lobular Liver Zonation Fibrosis in DILI and NASH Induced Liver Injury

Munish Puri *

Posted Date: 4 January 2024

doi: 10.20944/preprints202401.0361.v1

Keywords: DILI; NASH; liver zonation marker; bridging fibrosis; spatial transcriptomics; liver injury; computational biomarker; LSEC

Article

Spatial Computational Hepatic Molecular Biomarker Reveals LSECs Role in Mid Lobular Liver Zonation Fibrosis in DILI and NASH Induced Liver Injury

Munish Puri

Scientist, Onco-immunology, Machine learning, Magnit, CA USA; twishi03@gmail.com

Abstract: Liver is structurally organized into zonation where LSECs endothelial cells play a crucial role during chronic liver injury and early stages of fibrosis. Fibrosis can be reversed if diagnosed early at molecular level in zonation before progressing to advanced stages like bridging fibrosis. This study identified zonation marker genes using scRNA-seq and spatial transcriptomics molecular profiling technologies in normal and diseased fibrotic human liver. DEG analysis is performed over LSECs and identified the top 20 expressed genes in periportal, perivenous, and intermediate acinar zones. Multi-omics and scRNA-seq analysis over Visium images and ECs liver cells figured out *OIT3, DNASE1L3, CLEC4G, LYVE1, FCN2, CRHBP* as commonly expressed mid-lobular zonation-specific genes. Also, this study detected *STAB2, F8, AQP1, TEK, TIMP3, TIE1, CTSL* genes as expressed in DILI and NASH ECs populations. The connection between LSECs marker genes in zone 2 and liver fibrosis holds significant promise for advancing our understanding in developing new therapeutic strategies for fibrosis reversal and designing computational molecular biomarkers in NASH and DILI fibrotic liver diseases.

Keywords: DILI; NASH; liver zonation marker; bridging fibrosis; spatial transcriptomics; liver injury; computational biomarker; LSEC

1. Introduction

In a recent report, annually liver disease contributes around 4% of all the deaths worldwide and accounts for over two million deaths. The global burden of liver disease is placing a significant strain on public healthcare systems. Cirrhosis and Hepatocellular Carcinoma (HCC) are major contributors including Nonalcoholic fatty liver disease (NAFLD) and Drug-induced liver injury (DILI) which significantly contributes as common cause of liver related deaths[1].

The liver is the largest organ in the human body responsible for vital functions including metabolism of nutrients and xenobiotics. The liver is structurally made-up of small anatomical units called liver lobules. Every lobule is histologically organized in a unique hexagonal architectural arrangement of hepatocytes (parenchymal cells PCs) into three zones that exhibit a distinct functionality known as liver zonation. Venous blood from the gut mixes at portal vein with oxygenated atrial blood and flows towards central vein through sinusoids. The liver tissue area around portal triad i.e. peri-portal recognized as Zone1 (oxygen enriched) is involved in metabolic functions and specialized in gluconeogenesis whereas tissue area around central vein recognized as zone3 (less oxygen) is involved in bile acid production drug metabolism and glycolysis. The area in between i.e. mid-lobular known as Zone 2 is a transitional region where concentration of oxygenated blood, nutrients, metabolites, and gut-derived toxins varies along portal-central vein axis. Spatially heterogenous hepatocytes are distinguished by the gene expression profiles where 50% of the genes are expressed along lobular zonation axis[2]. Zone 2 is believed to plays an important role in homeostatic renewal of hepatocytes, liver mass regeneration and proliferation upon liver injury [3,4]. Spatial heterogeneity of parenchymal and non- parenchymal cells (NPCs) is zone dependent which

 doi:10.20944/preprints202401.0361.v1

modulate the Differentially Expressed Genes (GEGs) expression and initiate several liver diseases including Nonalcoholic steatohepatitis (NASH), DILI, HCC and liver regeneration[5].

Other than hepatocytes, Liver Sinusoidal Endothelial Cells (LSECs) contribute around 15–20% of total number of liver cells are highly specialized non parenchymal endothelial cells and act as a physical barrier between blood substrates and hepatocytes. Liver endothelial cells (ECs) includes LSEC, vascular ECs, and lymphatic ECs (LyECs)[6,7]. As chronic liver disease advances, hepatocyte functioning impaired by crosstalk between other liver cells which initiates an important role in regulating fibrosis. LSECs have unique fenestrae (pores) that allow for efficient clearance of pathogens, debris, and toxins from the blood, keeping the liver clean and functional. LSECs act as determinants of hepatic fibrosis where the process of capillarization precedes fibrosis in which LSECs lack fenestration and develop an organized basement membrane[8]. LSECs are the major drivers in fibrosis[9] and differential gene expression is observed between the different zones of the liver lobule during fibrosis[10]. For example, the periportal zone 1 expresses genes involved in the uptake of nutrients, mid-lobular zone2 expresses genes involved in metabolism of nutrients, pericentral zone 3 expresses genes involved in the secretion of bile. Gradient of differentially expressed genes (DEG) is observed in LSECs and hepatocytes following disrupted zonation architecture and liver functionalities in most liver diseases including NAFLD, NASH and DILI. DEG manifests around pericentral zone 3 that later progresses towards advanced stages of fibrosis, bridging fibrosis and cirrhosis [11,12]. Liver bridging fibrosis, a specific advanced NASH feature, is a type of scarring caused by the accumulation of excess collagen around hexagonal portal triad-central vein region in the later stages of liver fibrosis. These collagen bands connect different areas of the liver and block the flow of blood and bile, which leads to liver failure. Early liver fibrosis, a condition where scar tissue builds up, can indeed be reversed if detected early in zonation at molecular level and addressed promptly. However, it's crucial to remember that this reversal is contingent on preventing the progression to more advanced stages like bridging fibrosis, where the scar tissue becomes more organized, extensive and the damage is irreversible.

It's challenging to measure zonation-specific structural variations during early stages of fibrosis and later at bridging fibrosis level. Our knowledge is limited and poorly understood on the role of 1) zone 2 LSECs in early liver fibrosis, 2) LSECs-specific marker genes in hepatotoxic DILI conditions, 3) DEG profiles within unclear boundaries of liver zones under normal, NASH and DILI disease fibrotic patterns. In this study, efforts are made to computationally characterize and quantify spatial heterogeneity of hepatocytes at molecular level using single cell RNA seq and spatial molecular imaging techniques to develop our understanding of zonal restructuring, role of LSECs and marker genes in normal and diseased fibrotic conditions.

2. Results

2.1. Histopathology H&E Image Classification Experimental Workflow for Early and Bridging Fibrosis

Image analytics and experimental workflow, illustrated in Figure 1 D, is designed to classify Hematoxylin and Eosin (H&E) histopathology images under five categories i.e. normal, steatosis, early fibrosis, bridging fibrosis and cirrhosis. Machine learning widgets, shown in workflow, are executed to load, process, classify, cluster, and visualize the imaging data. After predictive analysis, images are clustered based on the common histologic disease features learned by the machine learning models, i.e. all the bridging fibrosis images grouped together under one group as shown in t-SNE plot Figure 1E and hierarchical clustering Figure 1B. Other category images are grouped similarly as per their disease morphology features. The Confusion matrix shown in Figure 1 F illustrates correctly predicted images (diagonally highlighted blocks) under respective categories. Closely clustered images share common morphological disease features in early fibrosis and steatosis (NASH specific feature) where white fat droplets are present in both images, shown as an example in Figure 1C. Classification models performance summarized in Table 1.

Preprints (www.preprints.org) | NOT PEER-REVIEWED | Posted: 4 January 2024 doi:10.20944/preprints202401.0361.v1

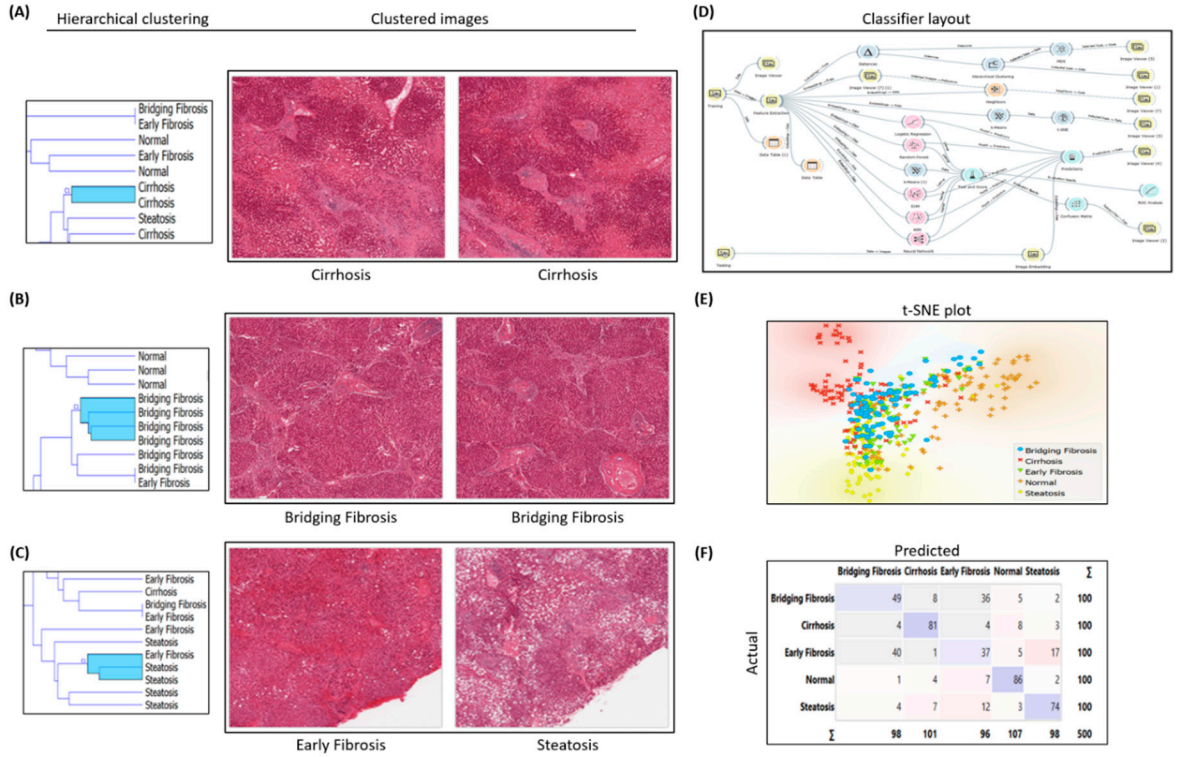

Figure 1. Experimental workflow, histopathology image classification & analysis; (A) H&E image classification for Cirrhosis; (B) Bridging Fibrosis; (C) Early Fibrosis & Steatosis; (D) Workflow of Classification experiment study design; (E) t-SNE plot for clustered images; (F) Confusion matrix of classifier performance.

Table 1.

Model	AUC	CA	F1	Precision	Recall
KNN	0.876	0.592	0.609	0.645	0.592
Tree	0.659	0.460	0.467	0.477	0.460
SVM	0.896	0.660	0.692	0.667	0.660
Random Forest	0.774	0.518	0.520	0.525	0.518
Neural Network	0.877	0.644	0.642	0.640	0.644
Naïve Bayes	0.847	0.600	0.597	0.598	0.600
Logistic Regression	0.892	0.656	0.655	0.654	0.656
Constant	0.500	0.200	0.067	0.040	0.582
AdaBoost	0.748	0.582	0.580	0.582	0.582

2.2. DEG Analysis for NASH and Zonation Expression

DEG analysis for NASH and zonation expression is performed over four independent studies *GSE89632, GSE126848, GSE83990, GSE105127* using NCBI GEO2R analysis tool. Volcano plots for NASH vs Control are illustrated in Figure 2A, zone1 vs zone 3 expression are illustrated in Figure 2B. Volcano plot displays statistical significance (-log10 P value) versus magnitude of change (log2 fold change) of differentially expressed genes in NASH vs control and zonation-specific expression studies. The most up regulated genes identified after analysis in NASH are *TYMS, FMO1, UQCRB*; and in zone1 vs zone 3 analysis are HAL, AQP1 KRT19. Details of DEGs and top up/down expressed genes are summarized in Table 2.

Preprints (www.preprints.org) | NOT PEER-REVIEWED | Posted: 4 January 2024 doi:10.20944/preprints202401.0361.v1

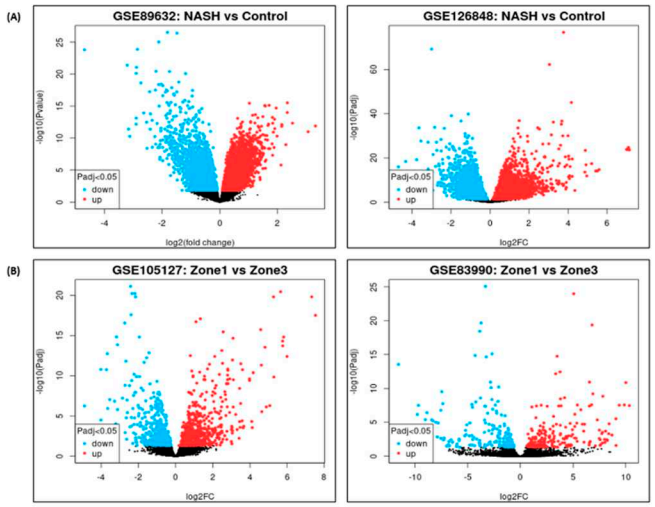

Figure 2. Volcano plots of Differential Gene Expression in; (A) NASH vs Control; (B) Zone 1 vs Zone 3.

Table 2.

NCBI GEO Study ID #	Publication PMID #	Year	Patients (N)	Differentially Expressed Genes (DEG)	Top UP/Down expressed genes
GSE89632	35166723	2016	NASH vs Healthy Control (N=63)	NASH vs Cntrl=2641 Steatosis vs Cntrl=3627 NASH vs Steatosis=11	Up=TYMS, FMO1; Down=MIR21, AXUD1 Up=FOSB, MYC; Down= RFXDC2, WNT5A Up= AKR1B10, CDC2; Down=IL6, CCL2
GSE126848	30653341	2019	NASH vs Healthy Control (N=45)	NASH vs Cntrl=1906 NAFLD vs Cntrl=1045 NASH vs NAFLD=5	Up=UQCRBP1, SNORD140; Down=FNBP1, GLUD1P2 Up=FNBP1, GLUD1P2; Down= UQCRBP1, SNORD140 Up=MRC2, GALNT18; Down= ST3GAL6, MAT1A
GSE83990	29244788	2018	Liver Zonation (N=12)	Zone1 vs Zone2=27 Zone2 vs Zone 3= 4 Zone1 vs Zone 3= 323	Up=DPT, STAB1; Down=OAT, SLCO1B3 Up=HAL, OIT3; Down=GLUL, SRPX Up=HAL, AQP1; Down=OAT, CXCL6
GSE105127	30297808	2018	Liver Zonation (N=57)	Zone1 vs Zone2=63 Zone2 vs Zone 3= 37 Zone1 vs Zone 3= 1010	Up=MGP, FGFR2; Down= TBX15, SLCO1B7 Up=SPRYD4, D9; Down=GLUL, PTGDS Up=KRT19, AQP1; Down=RSPO3, GLUL

2.3. Single Cell Clustering and DEGs Expression Profiles in DILI and NASH ECs

Single-cell transcriptomic analysis is performed over liver non-parenchymal cells (NPCs) in control, DILI and NASH datasets available at *NCBI GEO GSE166178*[13] and analyzed for the heterogeneity of inter- and intra-group endothelial cells in healthy and diseased mouse livers. Cell clustering results are illustrated in Figure 3A-B for control vs DILI, and control vs NASH illustrated in Figure 3C-D. DEGs expression is performed for eight commonly expressed genes *STAB2, OIT3, F8, AQP1, TEK, TIMP3, TIE1, CTSL* in DILI and NASH ECs populations, illustrated in Supplemental Figure S1

Preprints (www.preprints.org) | NOT PEER-REVIEWED | Posted: 4 January 2024 doi:10.20944/preprints202401.0361.v1

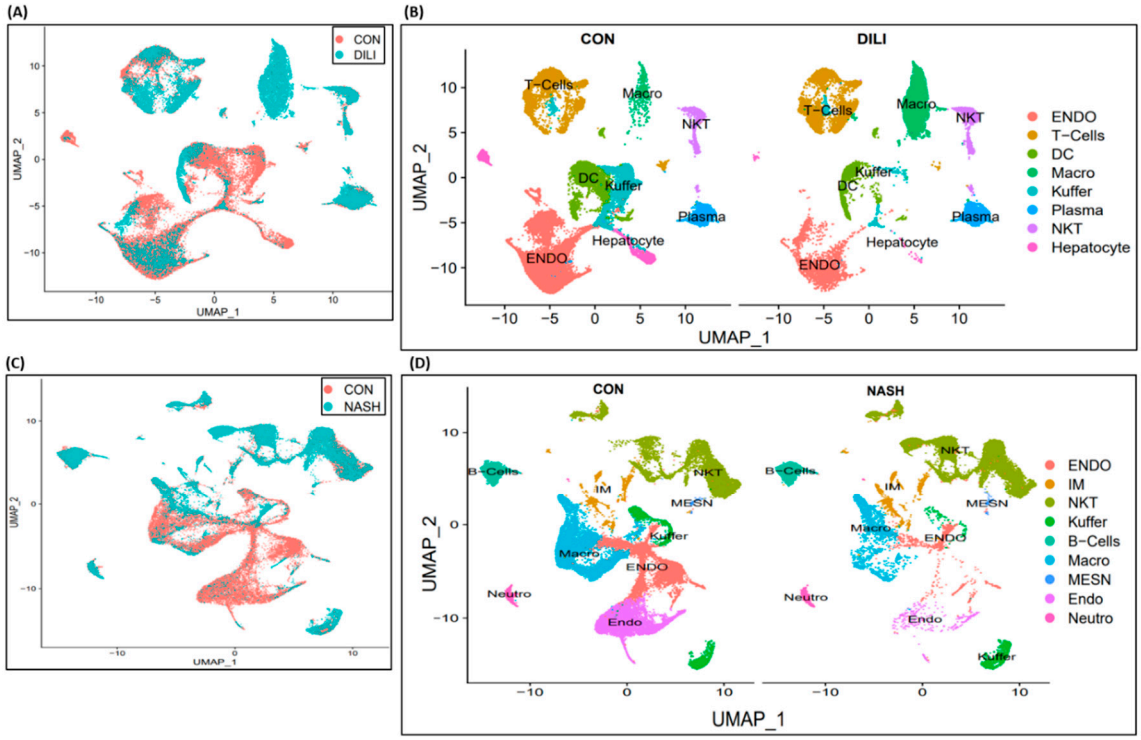

Figure 3. Single Cell clustering in DILI and NASH ECs (study GSE166178) (A) cell clustering for control & DILI samples (combined); (B) cell annotations and clustering(separately); (C) cell clustering for control & NASH samples(combined); (D) cell annotations and clustering(separately).

2.4. Spatial Transcriptomics Data Analysis for Zonation Marker Genes

2.4.1. 10x Genomics Visium Image Analysis for Spatial Distribution of Zonation Expression Markers

Spatial transcriptomics (ST) image analysis is performed on human liver H&E stained healthy and steatosis images using 10x genomic`s Visium platform to identify zonation patterns based on known markers[14]. Expressed dots(red) are the 55-micron Visium spots from where transcriptomes (RNA) are extracted for studying spatial cellular populations present and gene expressions at that specific tissue location. Figure 4A-4B illustrates zonation-specific expressed genes such as *HSPA1B, TIE1, OIT3, GLUL, HAL, SDS* overlaid Visium liver tissue image[15]. Expression profiles unraveled zonation patterns are highly dynamic varying from mild, mid to high in normal and steatosis samples.

Preprints (www.preprints.org) | NOT PEER-REVIEWED | Posted: 4 January 2024 doi:10.20944/preprints202401.0361.v1

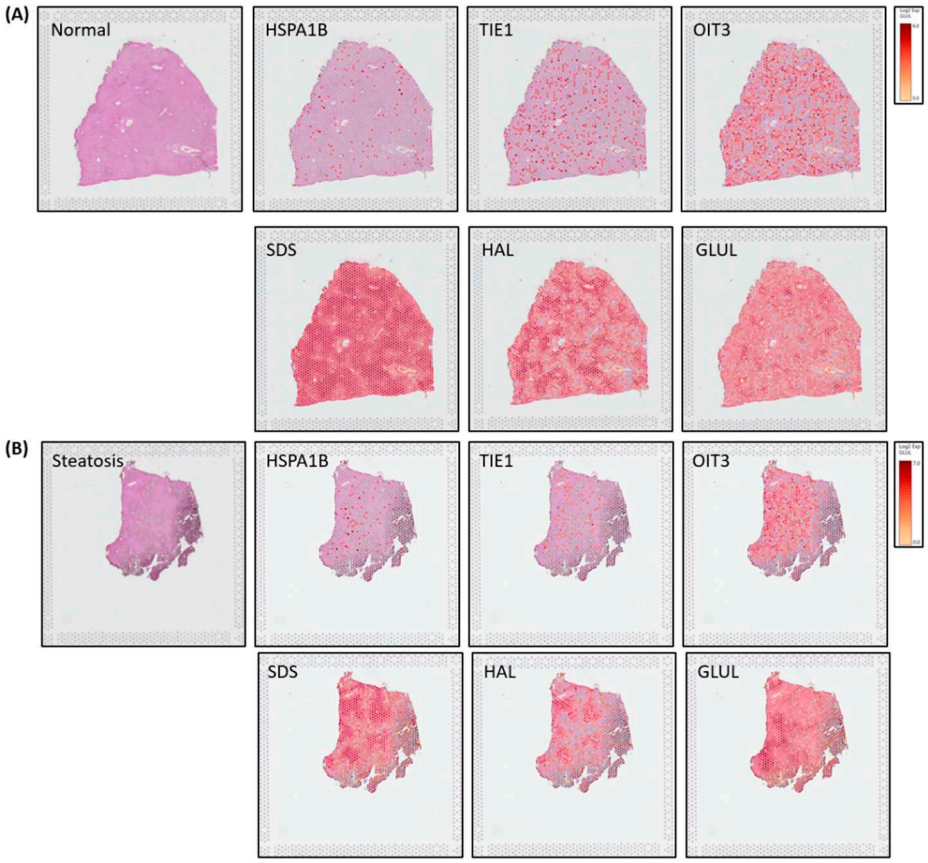

Figure 4. x genomics Visium image analysis for zonation marker in (A) Normal; (B) Steatosis.

2.4.2. Spatial Molecular Imaging to Demonstrate Liver Zonation Architecture

Nanostring`s CosMx™ Spatial Molecular Imager (SMI) platform, illustrated in Figure 5A is a high-plex spatial multiomics image generated from a 5 μm thick human formalin-fixed paraffin-embedded (FFPE) liver section stained for both protein and RNA analytes to demonstrate zone1, zone2 and zone 3 architecture. Figure 5B illustrates differential gene expression with three target markers i.e. *GLUL, FGG* & *SAA1* to highlight the zonation boundaries in a healthy liver tissue at molecular resolution. Similar equivalent patterns demonstrated in 10x genomics Visium images for the same three zonation-specific genes which highlights zonation boundaries in a normal human liver. However, in the diseased and chronic liver injury conditions, this zonation disruption exhibits varying DEG expression.

Preprints (www.preprints.org) | NOT PEER-REVIEWED | Posted: 4 January 2024 doi:10.20944/preprints202401.0361.v1

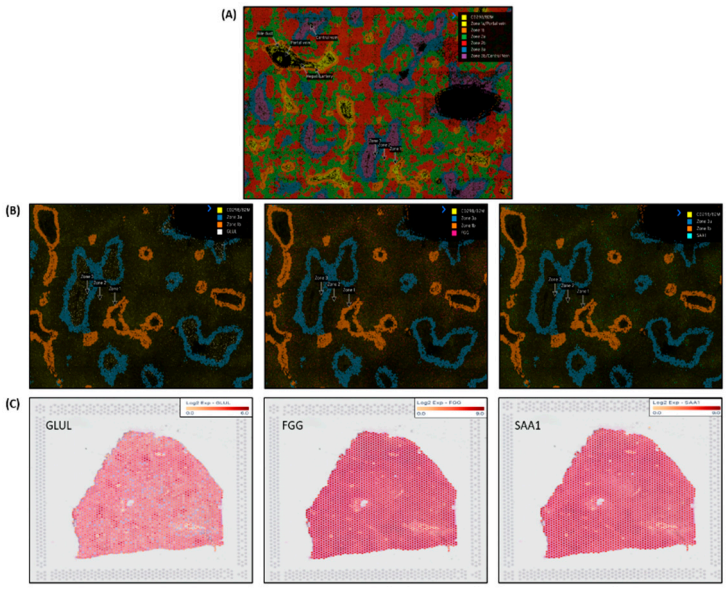

Figure 5. Nanostring`s CosMx Spatial Molecular Imager (SMI) of normal human liver demonstrates zonation architecture(A) Zonation boundaries for zone1,zone2,zone 3 and portal & central veins; (B) Zonation-specific gene expression, SAA1 as in zone1 (right), FGG as in zone 2 (middle) & GLUL as in zone 3 (left); (C) Similar zonation-specific expression demonstrated in Visium H&E image.

2.5. Liver Cell Clustering and LSECs Markers

Endothelial cell (ECs) clustering data analysis is executed here to demonstrate LSECs gene expression markers on an integrated scRNA-seq data of 28 healthy human liver samples. Single-cell scRNA-seq data used here was acquired from separate five independent studies reported elsewhere in [16]. Figure 6A illustrates UMAP clustering of all the normal liver cells. LSECs cluster shown in Figure 6B are picked as subset of clustered ECs cells shown in Figure 6A. Vascual Central Venous ECs (VCVEC) and Vascual Portal Venous ECs (VPEC) are clustered along-with LSECs, shown in Figure 6C which further separated as subsets and highlighted using ECs and LSECs separately with *CLEC4G*, *FCN2*, *OIT3*, *LYVE1* expression marker genes illustrated in Figure 6D-6E. VCVEC and VPEC clusters further separated and highlighted using *MGP*, *VWF*, *CD34* expression marker genes, illustrated in Figure 6F.

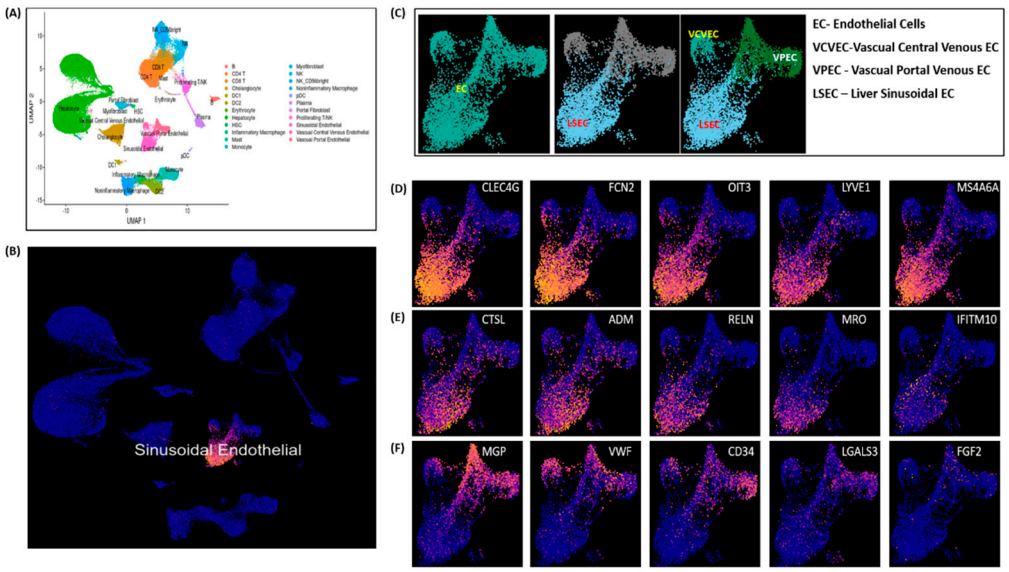

Preprints (www.preprints.org) | NOT PEER-REVIEWED | Posted: 4 January 2024 doi:10.20944/preprints202401.0361.v1

Figure 6. LSECs cell clustering and markers (A) clustering of all the normal liver cells; (B)LSECs cluster; (C) VCVEC, VPEC, LSECs subset under ECs cluster (D)-(E) LSECs marker gene expressions; (F) VCVEC and VPEC marker gene expression clusters.

2.6. DEG Expression Profiles in Zonated LSECs

DEG expression profiles identified the top 25 highly expressed genes with their marker score in PP–LSEC: Periportal Liver Sinusoid Endothelial Cells, PC–LSEC: Pericentral Liver Sinusoid Endothelial Cells and LSECs cells illustrated in Figure 7. A marker score is the 10th percentile of the effect sizes across all comparisons for each gene. DEG analysis is performed at cellxgene web-tool, a well curated, standardized, wide collection of interoperable single-cell transcriptomic data platform available at cellxgene.cziscience.com[17]. Five most commonly expressed genes *DNASE1L3*,*LIFR*,*STAB1*,*MRC1*,CRHBP are detected using cellxgene analysis and confirmed in another datasets[14]. Also, identified top 20 expressed genes in each zone are summarized in Table 3. Commonly expressed genes in this group are *MRC1, HAL, TIMP1* (zone1), *DNASE1L3, CRHBP*, *C9* (zone2) and *SELE, APOB, GLUL* (zone3). Their zonation-specific expression is confirmed using the human hepatocyte zonation browser tool, another open-source web platform publicly available web tool [18], illustrated in supplementary Figure S2.

Table 3.

Zone1	Zone2	Zone3
MRC1	DNASE1L3	SELE
HAL	CRHBP	APOB
TIMP1	C9	GLUL
SERPINE1	CDH5	FGF2
SAA1	IGFBP7	PLG
ID1	APOF	ITGA5
CLDN10	C8B	ICOS
CRP	LYVE1	PLPP3
SLPI	NOSTRIN	CTSS
CHI3L1	TTR	FGF2
FST	BTNL9	PLG
TIE1	ENG	LGR5
LGALS3	LIFR	NOTUM
TRAT1	FGG	SLC13A3
SDS	TEK	OAT
PDPN	KRT7	GPAM
ADAM23	CXCL6	SP5
FGFR2	LEPR	CYP2E1
H2AFY2	EDN1	SLCO1B3
RPL3	CD34	MTMR11

Preprints (www.preprints.org) | NOT PEER-REVIEWED | Posted: 4 January 2024 doi:10.20944/preprints202401.0361.v1

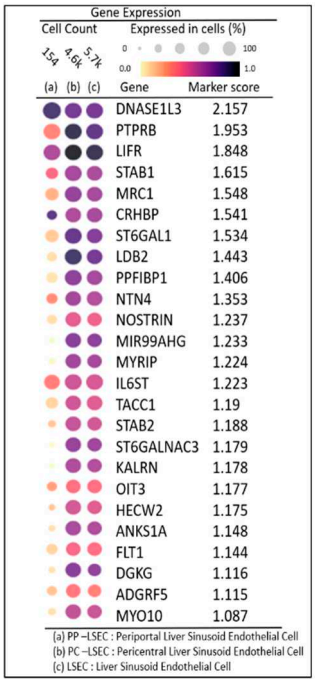

Figure 7. DEG expression profiles in PP–LSEC: Periportal Liver Sinusoid Endothelial Cells, PC–LSEC: Pericentral Liver Sinusoid Endothelial Cells and LSECs cells.

3. Discussion

In this study, efforts are made to develop our understanding towards complex interplay of LSECs in mid-lobular zone2 and their contributions in initiation of early fibrosis and regeneration. LSECs presence in zone 2 is influential and play a critical role in determining whether injured hepatocytes will regenerate or susceptible to fibrosis. Their anti-fibrotic ability to support regeneration is crucial for a successful liver repair process. LSECs secrete extracellular matrix (ECM) components like laminins, providing a supporting microenvironment for regeneration and ensuring proper tissue restructuring [19].

It's important to understand the zonation LSCEs functioning at cellular and molecular level and to quantify those architectural changes spatially in normal healthy and diseased liver conditions. Scarring tissue in NASH and DILI disease models exhibit common features of liver fibrosis. In this study, *OIT3* is computationally identified as commonly expressed marker gene in mid-lobular zone2 by LSECs cells population both in NASH and DILI datasets, which is also reported elsewhere in a study as a hallmark gene expressed in ECs [20]. The second most prominent gene identified is *DNASE1L3.* Other zonation-specific marker genes identified in our study are *MRC1, HAL* (zone1), *CRHBP, LYVE1*(zone2) and *SELE, GLUL* (zone3). Protein *F8* secreted by LSECs[21] plays important role in blood clotting is another marker gene detected in our experiment on *GSE166178 dataset* as highly expressed zone 2 marker gene and confirmed by zonation browser tool. Also found in this series *STAB2,CLEC4G, LYVE1* genes as mid-lobular zone 2 markers and confirmed as expressed healthy human liver[6,7].

The liver displays unique spatial heterogeneity and functioning of hepatocytes by exhibiting distinct metabolic and functional profiles across different acinar zones (periportal, perivenous, and intermediate). Specific enzymes, transporters, and other proteins act as zonation markers, reflecting the specialized functions of each zone. 10x genomic`s Visium platform and Nanostring's CosMx technologies used here to demonstrate these changes at molecular level and confirmed by zonation browser tool as the zonation-specific i.e. *GLUL* as zone3, *FGG* as zone2 and *SAA1* as zone 1 expressed marker genes.

DEG analysis of liver zonation can provide valuable insights into the mechanisms and potential therapeutic targets for fibrosis in NASH and DILI. In NASH related fibrosis, DEGs in Zone 1 might

 doi:10.20944/preprints202401.0361.v1

be related to lipid metabolism and oxidative stress, while Zone 3 DEGs could be involved in inflammation and bile acid signaling. Similarly in a specific DILI drug, DEGs might be related to mitochondrial dysfunction, immune response, or direct cell injury in specific zones. Fibrosis is caused by long-term chronic liver injury and is considered a hallmark disease feature of both NASH and DILI progression. This disrupts liver architecture and function, leading to potential organ failure. Different genes might be driving fibrosis in each zone, suggesting targeted therapies for each zonated area. DEGs could serve as early diagnostic or prognostic biomarkers for fibrosis progression in NASH and DILI. DEG analysis in NCBI GEO *GSE126848 study identified UQCRB* as the most up regulated gene in NASH and confirmed as a zone 2 marker, which is reported in a study elsewhere as molecular prognostic biomarker in human colorectal cancer[22]. DEG expression profiles identified five common expressed genes are as *DNASE1L3*, *LIFR*, *STAB1*, *MRC1*, CRHBP. Table summarized the top 25 highly expressed genes in PP–LSEC and PC-LSEC, such as *MRC1, HAL, TIMP1* (zone1), *DNASE1L3, CRHBP, C9* (zone2) and *SELE, APOB, GLUL* (zone3).

4. Methods and Materials

4.1. H&E Histopathology Image Classifications

Open-source visual programming data mining framework orange toolbox is used for classification of H&E histopathology image tiles. Orange is a machine learning data mining platform (http://orange.biolab.si) for image analysis and data visualization[23,24]. H&E stained Whole Slide (WSI) histopathology images were acquired from open-source National Cancer Institute (NCI) USA Biorepositories and Biospecimen Research Branch's (BBRB) Genotype-Tissue Expression (GTEx)Tissue Image library of annotated WSI with clinical data publicly available at https://brd.nci.nih.gov/brd/specimen/GTEX-117XS-0926 and downloaded under five categories as normal, steatosis, early fibrosis, bridging fibrosis & cirrhosis. Each WSI were cropped into tiles for training machine learning models and classified in orange tool classification layout. Experimental workflow is shown in Figure 1D.

4.2. Spatial Transcriptomics Data Analysis

4.2.1. Visium Data Analysis and Visualization

The Visium dataset used here is available at the Gene Expression Omnibus NCBI GEO public database under accession number GSE192742. Visium 10x genomics loupe browser image files downloaded from liver cell atlas available at https://www.livercellatlas.org/download.php The Visium ST images of normal and steatosis human liver samples were processed using Loupe Browser 7.0.1 (10x Genomics Inc.) downloaded from here https://www.10xgenomics.com/support/software/loupe-browser/downloads. The gene expression data for the k-mean clusters generated by the Space Ranger software for up regulated genes. The data consists of the median-normalized average of gene expression, log2 fold changes, and statistical significance (p values) computed for genes with a p value < 0.05.

4.2.2. Spatial Molecular Imaging

Spatial molecular imaging highlights DEG in human liver zonation. Imaging data were acquired from an open-source publicly available multiplex dataset at http://nanostring.com/CosMx-dataset CosMx™ Spatial Molecular Imager which includes staining for a panel of morphological features.

4.3. Liver Cell Clustering and Analysis Tool

For liver cell clustering and LSECs marker analysis, National Institute of Health`s (NIH) USA, Human BioMolecular Atlas Program (HuBMAP) Azimuth app is used. Azimuth is a Seurat based web application tool that uses an annotated reference dataset to automate the processing, analysis, and interpretation of single-cell RNA-seq data. Azimuth utilizes 'reference-based mapping' pipeline

 doi:10.20944/preprints202401.0361.v1

that accepts counts matrix file in multiple formats as input and performs normalization, visualization, cell annotation and DEG expression without any coding requirement on web cloud. All results can be visualized within the app, and can be downloadable for additional downstream analysis[25–29]. The development of Azimuth is led by the New York Genome Center Mapping Component as part of the NIH HuBMAP consortium.

4.4. LSECs Markers

Cellxgene Differential Expressed Gene (DEG) tool is used to run expression analysis for the cell types of PP-LSEC, PC-LSEC and LSECs cells. CellxGene is an open-source public database available at https://cellxgene.cziscience.com/ ; a suite of tools to run analysis of single-cell transcriptomic dataset. List of ECs expressed exclusively for LSECs cell populations are acquired from liver single cell expression atlas of 28 human livers[16] available at http://liveratlas-vilarinholab.med.yale.edu/ and plotted on LSECs HuBMAP Azimuth reference-based single-cell analysis tool for expression analysis. The analyzed results then compared with zonation browser tool to see the zonation profiles of same expressed genes in mid-lobular zone2. All three plots are illustrated in supplemental Figure S3. Zonation browser tool is available at https://itzkovitzwebapps.weizmann.ac.il/webapps/home/session.html?app=HumanandMouseHepatocyteZonation.

5. Conclusions

Mammalian healthy liver lobule is spatially well zonated and recognized with known markers based on distribution of metabolic functions that disrupts in diseased pathological conditions and liver injury. However, due to hepatocyte heterogeneity these zonation markers, such as enzymes, metabolites, and gene expression patterns vary in their expression and activity even within the same lobule. These molecular markers are not 1) zonation-specific; 2) disease -specific, for example, the expression and distribution of specific molecules within the liver changes during fibrogenesis in NASH and DILI. LSECs play an important and intricated role in the early stages of liver fibrosis and regeneration during mid-lobular zonation restructuring. Their strategic position allows them to act as critical conductors in influencing the delicate balance between tissue repair and scarring. Emerging trends in new technologies such as scRNA-seq, spatial transcriptomics and multiomics can be helpful to determine the role of LSECs in identifying the zonation marker DEGs at cellular and molecular level. LSCEs can provide valuable insights into how zonation marker variations and fibrosis are interconnected. This study identified zonation-specific mid-lobular markers of LSECs. Liver fibrosis in early stages can be reversible if detected in zonation at molecular level before moving to advanced stages like bridging fibrosis. Current diagnostic methods often lack accuracy at early stages of liver fibrosis. This is where computational biomarkers derived from integrated multi-omics, cellular and molecular data hold immense promise for providing a deeper understanding and improved diagnosis of liver fibrosis. The limitation of this study is that DEG analysis alone is not sufficient to understand early stages of fibrosis in complex diseases like NASH and DILI. Integrating it with other data, such as protein expression and metabolic profiling is required to analyze in normal and diseased conditions. More research is needed to validate DEGs as reliable zonation markers and translate them into effective diagnostic and prognostic biomarkers. Investigating LSCEs in the context of both zonation and fibrosis holds significant promise for developing novel therapeutic strategies against liver diseases. This may help to protect zonation patterns, prevent fibrosis development, and ultimately improve liver health.

Supplementary Materials: The following supporting information can be downloaded at the website of this paper posted on Preprints.org.

Conflicts of Interest: No conflict of interest.

References

1. Devarbhavi, H.; Asrani, S.K.; Arab, J.P.; Nartey, Y.A.; Pose, E.; Kamath, P.S. Global Burden of Liver Disease: 2023 Update. *J. Hepatol.* **2023**, *79*, 516–537, doi:10.1016/j.jhep.2023.03.017.
2. Ben-Moshe, S.; Itzkovitz, S. Spatial Heterogeneity in the Mammalian Liver. *Nat. Rev. Gastroenterol. Hepatol.* **2019**, *16*, 395–410, doi:10.1038/s41575-019-0134-x.
3. Itoh, T. The Truth Lies Somewhere in the Middle: The Cells Responsible for Liver Tissue Maintenance Finally Identified. *Cell Regen. Lond. Engl.* **2021**, *10*, 28, doi:10.1186/s13619-021-00090-8.
4. Wei, Y.; Wang, Y.G.; Jia, Y.; Li, L.; Yoon, J.; Zhang, S.; Wang, Z.; Zhang, Y.; Zhu, M.; Sharma, T.; et al. Liver Homeostasis Is Maintained by Midlobular Zone 2 Hepatocytes. *Science* **2021**, *371*, eabb1625, doi:10.1126/science.abb1625.
5. Panday, R.; Monckton, C.P.; Khetani, S.R. The Role of Liver Zonation in Physiology, Regeneration, and Disease. *Semin. Liver Dis.* **2022**, *42*, 001–016, doi:10.1055/s-0041-1742279.
6. Verhulst, S.; van Os, E.A.; De Smet, V.; Eysackers, N.; Mannaerts, I.; van Grunsven, L.A. Gene Signatures Detect Damaged Liver Sinusoidal Endothelial Cells in Chronic Liver Diseases. *Front. Med.* **2021**, *8*, 750044, doi:10.3389/fmed.2021.750044.
7. Su, T.; Yang, Y.; Lai, S.; Jeong, J.; Jung, Y.; McConnell, M.; Utsumi, T.; Iwakiri, Y. Single-Cell Transcriptomics Reveals Zone-Specific Alterations of Liver Sinusoidal Endothelial Cells in Cirrhosis. *Cell. Mol. Gastroenterol. Hepatol.* **2021**, *11*, 1139–1161, doi:10.1016/j.jcmgh.2020.12.007.
8. DeLeve, L.D. Liver Sinusoidal Endothelial Cells in Hepatic Fibrosis. *Hepatol. Baltim. Md* **2015**, *61*, 1740–1746, doi:10.1002/hep.27376.
9. Lafoz, E.; Ruart, M.; Anton, A.; Oncins, A.; Hernández-Gea, V. The Endothelium as a Driver of Liver Fibrosis and Regeneration. *Cells* **2020**, *9*, 929, doi:10.3390/cells9040929.
10. Ghallab, A.; Myllys, M.; H. Holland, C.; Zaza, A.; Murad, W.; Hassan, R.; A. Ahmed, Y.; Abbas, T.; A. Abdelrahim, E.; Schneider, K.M.; et al. Influence of Liver Fibrosis on Lobular Zonation. *Cells* **2019**, *8*, 1556, doi:10.3390/cells8121556.
11. Nagy, D.; Maude, H.; Birdsey, G.M.; Randi, A.M.; Cebola, I. RISING STARS: Liver Sinusoidal Endothelial Transcription Factors in Metabolic Homeostasis and Disease. *J. Mol. Endocrinol.* **2023**, *71*, doi:10.1530/JME-23-0026.
12. Ben-Moshe, S.; Veg, T.; Manco, R.; Dan, S.; Papinutti, D.; Lifshitz, A.; Kolodziejczyk, A.A.; Halpern, K.B.; Elinav, E.; Itzkovitz, S. The Spatiotemporal Program of Zonal Liver Regeneration Following Acute Injury. *Cell Stem Cell* **2022**, *29*, 973-989.e10, doi:10.1016/j.stem.2022.04.008.
13. Wang, Z.; Qian, J.; Lu, X.; Zhang, P.; Guo, R.; Lou, H.; Zhang, S.; Yang, J.; Fan, X. *A Single-Cell Transcriptomic Atlas Characterizes Liver Non-Parenchymal Cells in Healthy and Diseased Mice*; Genomics, 2021;
14. Halpern, K.B.; Shenhav, R.; Matcovitch-Natan, O.; Tóth, B.; Lemze, D.; Golan, M.; Massasa, E.E.; Baydatch, S.; Landen, S.; Moor, A.E.; et al. Single-Cell Spatial Reconstruction Reveals Global Division of Labour in the Mammalian Liver. *Nature* **2017**, *542*, 352–356, doi:10.1038/nature21065.
15. Hildebrandt, F.; Andersson, A.; Saarenpää, S.; Larsson, L.; Van Hul, N.; Kanatani, S.; Masek, J.; Ellis, E.; Barragan, A.; Mollbrink, A.; et al. Spatial Transcriptomics to Define Transcriptional Patterns of Zonation and Structural Components in the Mouse Liver. *Nat. Commun.* **2021**, *12*, 7046, doi:10.1038/s41467-021-27354-w.
16. Brancale, J.; Vilarinho, S. A Single Cell Gene Expression Atlas of 28 Human Livers. *J. Hepatol.* **2021**, *75*, 219–220, doi:10.1016/j.jhep.2021.03.005.
17. Program, C.S.-C.B.; Abdulla, S.; Aevermann, B.; Assis, P.; Badajoz, S.; Bell, S.M.; Bezzi, E.; Cakir, B.; Chaffer, J.; Chambers, S.; et al. CZ CELL×GENE Discover: A Single-Cell Data Platform for Scalable Exploration, Analysis and Modeling of Aggregated Data 2023, 2023.10.30.563174.
18. Massalha, H.; Bahar Halpern, K.; Abu-Gazala, S.; Jana, T.; Massasa, E.E.; Moor, A.E.; Buchauer, L.; Rozenberg, M.; Pikarsky, E.; Amit, I.; et al. A Single Cell Atlas of the Human Liver Tumor Microenvironment. *Mol. Syst. Biol.* **2020**, *16*, e9682, doi:10.15252/msb.20209682.
19. Natarajan, V.; Harris, E.N.; Kidambi, S. SECs (Sinusoidal Endothelial Cells), Liver Microenvironment, and Fibrosis. *BioMed Res. Int.* **2017**, *2017*, 4097205, doi:10.1155/2017/4097205.
20. Li, Z.-W.; Ruan, B.; Yang, P.-J.; Liu, J.-J.; Song, P.; Duan, J.-L.; Wang, L. Oit3, a Promising Hallmark Gene for Targeting Liver Sinusoidal Endothelial Cells. *Signal Transduct. Target. Ther.* **2023**, *8*, 1–10, doi:10.1038/s41392-023-01621-2.
21. Jamil, M.A.; Singer, H.; Al-Rifai, R.; Nüsgen, N.; Rath, M.; Strauss, S.; Andreou, I.; Oldenburg, J.; El-Maarri, O. Molecular Analysis of Fetal and Adult Primary Human Liver Sinusoidal Endothelial Cells: A Comparison to Other Endothelial Cells. *Int. J. Mol. Sci.* **2020**, *21*, 7776, doi:10.3390/ijms21207776.
22. Kim, H.-C.; Chang, J.; Lee, H.S.; Kwon, H.J. Mitochondrial UQCRB as a New Molecular Prognostic Biomarker of Human Colorectal Cancer. *Exp. Mol. Med.* **2017**, *49*, e391, doi:10.1038/emm.2017.152.
23. Demšar, J.; Curk, T.; Erjavec, A.; Gorup, Č.; Hočevar, T.; Milutinovič, M.; Možina, M.; Polajnar, M.; Toplak, M.; Starič, A.; et al. Orange: Data Mining Toolbox in Python. *J. Mach. Learn. Res.* **2013**, *14*, 2349–2353.

24. Godec, P.; Pančur, M.; Ilenič, N.; Čopar, A.; Stražar, M.; Erjavec, A.; Pretnar, A.; Demšar, J.; Starič, A.; Toplak, M.; et al. Democratized Image Analytics by Visual Programming through Integration of Deep Models and Small-Scale Machine Learning. *Nat. Commun.* **2019**, *10*, 4551, doi:10.1038/s41467-019-12397-x.
25. Hao, Y.; Hao, S.; Andersen-Nissen, E.; Mauck, W.M.; Zheng, S.; Butler, A.; Lee, M.J.; Wilk, A.J.; Darby, C.; Zager, M.; et al. Integrated Analysis of Multimodal Single-Cell Data. *Cell* **2021**, *184*, 3573-3587.e29, doi:10.1016/j.cell.2021.04.048.
26. Aizarani, N.; Saviano, A.; Sagar; Mailly, L.; Durand, S.; Herman, J.S.; Pessaux, P.; Baumert, T.F.; Grün, D. A Human Liver Cell Atlas Reveals Heterogeneity and Epithelial Progenitors. *Nature* **2019**, *572*, 199–204, doi:10.1038/s41586-019-1373-2.
27. Ramachandran, P.; Dobie, R.; Wilson-Kanamori, J.R.; Dora, E.F.; Henderson, B.E.P.; Luu, N.T.; Portman, J.R.; Matchett, K.P.; Brice, M.; Marwick, J.A.; et al. Resolving the Fibrotic Niche of Human Liver Cirrhosis at Single-Cell Level. *Nature* **2019**, *575*, 512–518, doi:10.1038/s41586-019-1631-3.
28. Zhang, M.; Yang, H.; Wan, L.; Wang, Z.; Wang, H.; Ge, C.; Liu, Y.; Hao, Y.; Zhang, D.; Shi, G.; et al. Single-Cell Transcriptomic Architecture and Intercellular Crosstalk of Human Intrahepatic Cholangiocarcinoma. *J. Hepatol.* **2020**, *73*, 1118–1130, doi:10.1016/j.jhep.2020.05.039.
29. MacParland, S.A.; Liu, J.C.; Ma, X.-Z.; Innes, B.T.; Bartczak, A.M.; Gage, B.K.; Manuel, J.; Khuu, N.; Echeverri, J.; Linares, I.; et al. Single Cell RNA Sequencing of Human Liver Reveals Distinct Intrahepatic Macrophage Populations. *Nat. Commun.* **2018**, *9*, 4383, doi:10.1038/s41467-018-06318-7.